IOSR Journal of Computer Engineering (IOSR-JCE)
e-ISSN: 2278-0661,p-ISSN: 2278-8727, Volume 23, Issue 6, Ser. I (Nov. –Dec. 2021), PP 29-34
www.iosrjournals.org

Finding Similarity between the Left and Right Retinal Images of an Individual Using Legendre Moments

Md. Iqbal Aziz Khan, Md Rokanujjaman, Md. Tanvir Hossain, Sangeeta Biswas
(Department of Computer Science and Engineering, University of Rajshahi, Bangladesh)

Abstract: *Many researchers in medical science studied the similarity between the left and right retina of a patient. On the contrary, many retina-based biometric researchers consider that an individual's left and right retinas are different. Therefore, few works were reported in retina-based biometric for finding similarities between the left and right retina of an individual. This research intends to find similarities between an individual's left and right retina using orthogonal Legendre moments from a biometric perspective. Here, we use orthogonal Legendre moments for feature extraction and dimensionality reduction and cosine distance to measure similarity between the Legendre moments-based vectors extracted from the left and right retina. We perform experiments on two publicly available data sets named CHASE_DB1 and Messidor-2. We show that the Legendre moments can preserve almost all the retinal image information in few coefficients, and there exists a noticeable similarity in the Legendre moments extracted from the left and right retinal images of an individual.*

Key Word*: Legendre moments, retina, cosine similarity, biometric.*

Date of Submission: 12-11-2021 Date of Acceptance: 28-11-2021

I. Introduction

The retina is a neural tissue that helps to form images in our brain by converting electromagnetic signals into neural signals. It plays an important role both in our vision and biometric. Pathology in the retina can be the cause of irreversible partial or complete vision loss. Therefore, patients' retina is one of the focusing points for ophthalmologists, medical researchers, and computer-aided diagnostic devices. The tree structure of the central retinal blood vessels remains unchanged during a person's lifetime unless being affected by severe retinal pathology. The external environment cannot affect it since its location is inside our eye [1]. Therefore, the retina was studied as a reliable biometric to ensure high security in an environment with massive interest by biometric researchers since 1899 [2-19].

The similarity between the left and right retina can benefit medical science in two ways. First, it allows ophthalmologists to use one retina as a proxy for the other retina during the post-surgery and post-treatment analysis. Second, it helps to track pathology progress in a retina compared to the other retina. If two retinas have any similar anatomical feature, then dissimilarity in that feature indicates pathology development in the retina. For example, the presence of unevenness between the optic nerve cup of the two eyes of an individual is considered an early sign of glaucomatous damage [20][21] and is a predictor of future damage in ocular hypertensive patients [22]. Therefore, many researchers explored the similarity between the left and right retina in many works in medical science [23-28].

On the contrary, few researchers worked on the similarity issue between the left and right retina from a biometric perspective. Except for the works done by Biswas and her colleagues, no other works can be found in the literature regarding this issue. Biswas et al. turned the problem of finding the similarity in the left and right retina into a verification problem and reported experimental results in [29-33]. If a system (either human or a machine learning algorithm) decided that a pair of retinal images of the left and right retinas was captured from a single subject, they assumed that the system found substantial similarity in that pair. On the other hand, if the system decided that a pair of left and right retinas belongs to two different subjects, they assumed that the system did not see any similar properties in that pair. By manual and automatic verification, they investigated to what extent their assumptions are correct in [29-33]. In [29], [34] Biswas et al. also discussed the similarity between left and right retina as an identification problem. They assumed that if the left and right retinas, captured from a single subject, then the pair of the left and right retinal images would have lower cosine distance or higher cosine similarity compared to the pairs made by taking a left and right retinal images from two different subjects. The cosine similarity can be easily measured after reshaping two 2D images of blood vessels or 3D RGB retinal images to vectors. However, these vectors are so long that the cosine similarity suffers from the curse of high dimensionality. Before measuring the cosine similarity, two neural network-based embedding techniques along with three non-neural network-based embedding techniques were investigated to

reduce dimension: principal component analysis (PCA), locally linear embedding (LLE), and isometric mapping (Isomap). Embedding is a mapping of a high dimensional variable into a low dimensional variable.

This research aims to explore a Legendre moments based non-neural network-based feature other than PCA, LLE and Isomap for finding similarities between an individual's left and right retinas. The Legendre moments are orthogonal and scale, translation and rotation invariant. Hence, they represent various features of the retina. However, finding the best set of Legendre moments for assessing the degree of similarities between an individual's left and right retinas is very challenging.

We organize this paper as follows. In Section 2, we describe briefly Legendre moments. Then in Section 3, we describe data sets that we use in experiments. We devote Section 4 to the cosine distance-based similarity measurement between Legendre moments based features extracted from the left and right retina. We present evaluation results in Section 5. Finally, concluding remarks are given in Section 6.

II. Legendre Moments

Legendre moments are used in a lot of image processing and pattern recognition applications such as blurred image recognition [35]. They belong to the class of orthogonal moments. They use Legendre polynomials as basis set. The two-dimensional Legendre moments of order *(p, q)*, with an image intensity function *f(x, y)*, are defined on the square [-1, 1] × [-1, 1] as

$$L_{pq} = \lambda_{pq} \iint_{-1}^{1} P_p(x) P_q(y) f(x,y) dxdy \tag{1}$$

where $\lambda_{pq} = \frac{(2p+1)(2q+1)}{4}$, *p, q = 0, 1, 2, ..., ∞,* and $P_p(x)$ is the p_{th} order Legendre polynomial defined by

$$P_p(x) = \sum_{k=0}^{p} \left\{ \frac{(-1)^{\frac{p-k}{2}} x^k (p+k)!}{2^p k! \left(\frac{p-k}{2}\right)! \left(\frac{p+k}{2}\right)!} \right\}, p-k = even \tag{2}$$

And, the recurrent formula of Legendre polynomials is

$$\begin{cases} P_{p+1}(x) = \dfrac{2p+1}{p+1} x P_p(x) - \dfrac{p}{p+1} P_{p-1}(x) \\ P_1(x) = x, P_0(x) = 1 \end{cases} \tag{3}$$

The Legendre polynomials are a complete orthogonal basis set on the interval [-1, 1]. The relation of orthogonality is defined as

$$\int_{-1}^{1} P_p(x) P_q(x) dx = \frac{2}{2p+1} \delta_{pq} \tag{4}$$

where,

$\delta_{pq} = \begin{cases} 1 & if p = q \\ 0 & if p \neq q \end{cases}$ is the Kronecker symbol.

The orthogonal property of Legendre polynomials implies no redundancy or overlapping of information between the moments with different orders. This property enables the contribution of each moment to be unique and independent from the information in an image [36].

To compute Legendre moments of a digital image, the integrals in Equation (1) are replaced by summations and the coordinates of the image are normalized into [-1, 1]. Therefore, the numerical approximate form of Legendre moments, for a discrete image of $M \times N$ pixels with image intensity function $f(x, y)$, is [37]

$$L_{pq} = \lambda_{pq} \sum_{i=0}^{M-1} \sum_{j=0}^{N-1} P_p(x_i) P_q(y_j) f(x_i, y_j) \tag{5}$$

where $\lambda_{pq} = \frac{(2p+1)(2q+1)}{M \times N}$, x_i and y_j denote the normalized pixel coordinates in the range of [-1, 1].

III. Data Sets

The publicly available retina data sets are mainly prepared for tasks other than finding similarities between an individual's left and right retina, e.g., automatic pathology detection; segmentation of anatomical structures such as optic disc, macula, and central retinal blood vessels; assessing the image quality; and retinal image registration. Most of the data sets have images from only one side and one session. Therefore, most of the data sets are not appropriate for our purpose. Few data sets have images from both side retinas, among which we choose two data sets to do the identification: (1) Child Heart Health Study in England (CHASE) data set and (2) Methods to Evaluate Segmentation and Indexing Techniques in the field of Retinal Ophthalmology-2 (Messidor-2) data sets. These two public data sets have a pair of left and right retinal images per subject. Two example pairs of these data sets are shown in Figure 1.

CHASE_DB1 [38], [39] contains 14 pairs of colored retinal images (i.e., 28 RGB retinal images in total), captured by a Hand-held Nidek NM-200-D camera, with 999×960 pixels. It is a subset of retinal images captured from multi-ethnic children.

Messidor-2 [40] contains 874 pairs of images captured from the left and right retina of 874 subjects using a Topcon TRC NW6 non-mydriatic fundus camera with a 45-degree field of view having 1440x960, 2240x1488, and 2304x1536 pixels.

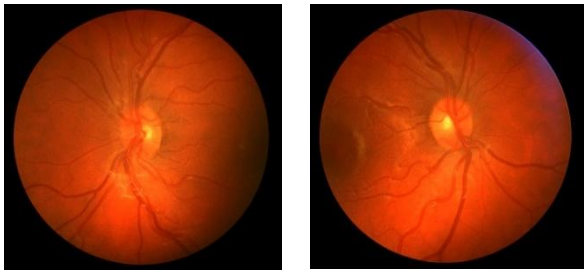

(a) CHASE_DB1

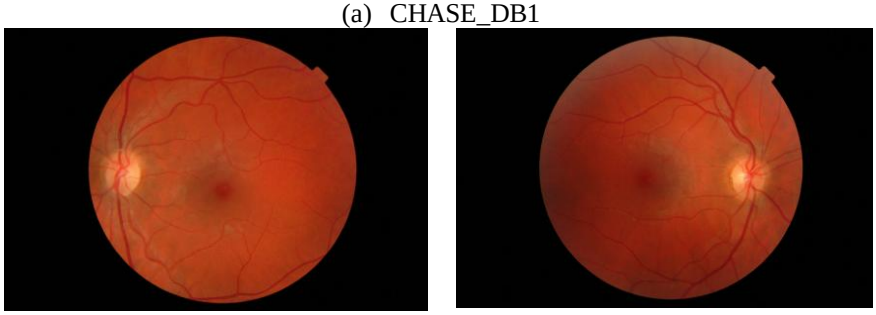

(b) Messidor-2

Figure 1: Two Example Pairs of Left and Right Retinal Images of the Datasets (a) CHASE_DB1 and (b) Messidor-2

IV. Legendre Moments based Similarity Measurement

At first we convert each 3D RGB retinal images of a data set (i.e., CHASE_DB1 and Messidor-2) into 2D grayscale images by performing a weighted summation of three color channels in the following way

Grayscale = 0.299 x Red + 0.587 x Green + 0.114 x Blue.

Except that no other preprocessing (such as image enhancement, background cropping, or denoising) is done on any retinal image. After that we represent each grayscaled retinal image by a sequence of Legendre moments L_S, $\{L_0, L_{1,} Z_2, L_3 \dots L_S\}$ where S is the order of the moments. We set $S = 15$ assuming that the computation of cosine distance between the low dimensional Legendre feature vectors will not suffer from the curse of high dimensionality.

Two sample left retinal images and one right retinal image of the CHASE_DB1 data set along with their corresponding 15 order Legendre moments are shown in Table 1.

Table 1: Fifteen Legendre Moments of Two Left and One Right Retinal Images

Retina	Image	Legendre moments
Left1	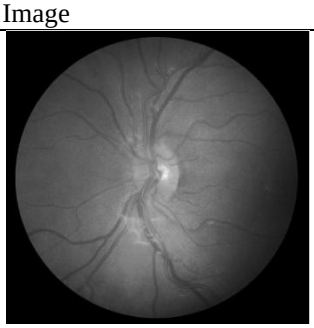	-2.54883216644013, -39.1841405357075, 0.519517186326675, 1.09555006610562, -0.195206187674502, -0.024244949300752, 0.001774621167093, -0.111701953187058, 0.042335373583012, 0.068560284172142, -0.019016578815481, 0.112713784523971, 0.014495142325508, 0.229014184160956, -0.016658880384136

Right1	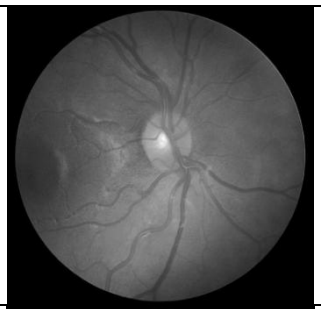	-2.44195690601696, -40.1609229725178, 0.465676337493098, 0.251467346822934, 0.2029634304591, -0.401027841891579, -0.249114685951248, 0.152025985269091, 0.120675467962824, -0.002092193401076, -0.10904412968962, 0.079295887598107, 0.063789838410484, 0.269551196825741, -0.05992901829815
Left5	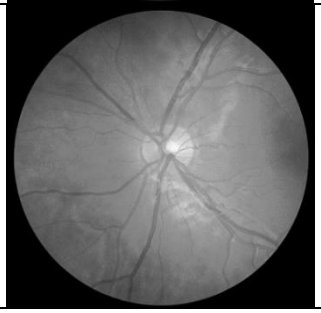	0.14553990681233, -54.815478285092, -0.233357897290385, 2.34639643397884, 0.159220891497932, -1.07689549183256, -0.141497894945793, 0.284929316863294, 0.06730653926678, 0.069482533010556, -0.046496802781095, 0.004889504051136, -0.022685093949874, 0.327549539105079, -0.016335496559562

After extracting orthogonal Legendre moments based feature vectors for all the left and right retinal images of a data set, we estimate the cosine distance for each possible pair of left and right retina in the following way

$$\cos\theta = \frac{\vec{L}\cdot\vec{R}}{\|\vec{L}\|\|\vec{R}\|} = \frac{\sum_{i=1}^{n} L_i R_i}{\sqrt{\sum_{i=1}^{n} L_i^2}\sqrt{\sum_{i=1}^{n} R_i^2}} \tag{6}$$

where $\vec{L}\cdot\vec{R}$ is the dot product between the Legendre feature vector of the left and right retina and n is the dimension of the vectors. The cosine distance between five pairs of left and right retinal images of CHASE_DB1 are shown in Table 2. Each diagonal cell belongs to a pair of left and right retinal images from a single subject, whereas each non-diagonal cell belongs to a pair of left and right retinal images from two different subjects. The smallest value in the first diagonal cell indicates that the correct right retina (i.e., Right1) has the smallest cosine distance with the left retina (i.e., Left1). It means that the left retina (i.e., Left1) of Subject1 is more similar to the right retina of Subject1 (i.e., Right1) than the right retinas of other subjects (i.e., Subject2, Subject3, Subject4, and Subject5). Same thing happens to Left2, Left3, and Left4. Such cases are the examples of correctly identified right retinas for left retinas. The ideal case is that all diagonal cells of Table 2 have the smallest cosine distance comparing to other cosine distances in that row. However, for Left5 it happens that the smallest value is not in the diagonal cell. In the fifth row (i.e., for L5 retina), the smallest cosine distance is found in the first cell, i.e., with R1 retina. Such case is an example of wrongly recognized right retina for a left retina.

We investigate for how many left retinas can find the smallest cosine distance in k nearest neighbors of right retinas. There is a correspondence between the value of k and the degree of similarity. Smallest value of k represents a high degree of similarity. In contrast, largest value reports a low degree of similarity.

Table 2: Cosine Distances Measured between the Left (L) and Right (R) Retinal Images.

Right / Left	Right1	Right2	Right3	Right4	Right5
Left1	**0.00038761**	0.00273396	0.00443778	0.00421216	0.00556403
Left2	0.00781619	**0.00112177**	0.00865895	0.00128904	0.00218104
Left3	0.00060657	0.00459435	**0.00013687**	0.00050906	0.00767014
Left4	0.00177693	0.00688795	0.00656728	**0.00091488**	0.00123844
Left5	**0.00054917**	0.00089887	0.00078071	0.00065637	0.00109431

V. Results and Discussion

It is found in the experiments that the lower orders of Legendre moments mainly contain fundamental retinal image information, while the higher orders of Legendre moments preserve more detailed retinal image information. Only lower-order or only higher-order moments have few significant effects on the similarities

measurement. A set of both lower-order and higher-order moments is taken from the whole retinal image. However, it is experimentally observed that all the parts in the whole image cannot contribute equally. Part-based Legendre moments are calculated from both retinas of an individual and from the two different persons. In most of the cases similar or very close Legendre moments are found from the same parts of the left and right retinas of an individual based on cosine distance. On the other hand, different Legendre moments are found from the same parts of the two different persons' eyes. Moreover, in some cases Legendre moments of some parts in the left and right retinal images of an individual cannot influence our similarity assessment task. Part-based Legendre moments are not used in this work.

The probability of finding the correct right retina among the k-nearest right retinas for a left retina is shown in Table 3. Note that the probability of retrieving the correct right retina for a left retina by chance is 1/14 = 0.0714 for CHASE_DB1 and 1/874 = 0.0011 for Messidor-2. As shown in Table 3, the probability of retrieving the correct right retina for a left retina is 0.61 for CHASE_DB1 and 0.22 for Mesidor-2, respectively. Among five nearest neighbors, the probability of being the actual right retina for a left retina is 0.92 and 0.71, respectively. These values are much higher than by chance. It indicates that a subject's left and right retinas have more similarities than those from two different subjects. There is a significant difference in the performances of the two datasets. One reason behind this phenomenon might be the size difference of the two datasets. As the number of subjects increases, it becomes increasingly difficult for the system to accurately find the right retina for a left retina.

Table 3: Probability of Finding Similarity of Left Retina in k-nearest Right Retinas

Dataset	Values of k	Probability
CHASE_DB1	1, 2, 3, 4, 5	0.61, 0.82, 0.89, 0.91, 0.92
Messidor-2	1, 2, 3, 4, 5	0.22, 0.34, 0.53, 0.6, 0.71

VI. Conclusion

In this paper, for the first time, we have shown that the orthogonal Legendre moments can be used as a feature vector to find substantial similarity between the left and right retinal images captured from a single subject. We perform experiments on two publicly available data sets (i.e., CHASE_DB1 and Messidor-2) with a pair of left and right retina for each subject. By estimating orthogonal moments for both left and right retinal images at first and then estimating cosine distance between estimated moments, we have shown that a left retina has the lowest cosine distance from a right retina when they are from the same subject than when they are from two different subjects. Performing experiments on a database having more pairs of left and right retinal images than the Messidor-2 (i.e., more pairs than 874 pairs) and multiple pairs for each subject captured in different settings is necessary for figuring out more exciting information about the similarity of an individual's left and right retina. This task can be a good research direction in the future.

References

[1]. K. Jain, R. Bolle, and S. Pankanti, Eds., "Retina Identification", Springer US, 1996, pp. 123–141.

[2]. S. Türkel, "Das Auge als Identifizierungsgrundlage: Unter Berücksichti-gung von Blascheks Photofundoskopie," Slack Incorporated, 1927, ch. III, pp. 22–41.

[3]. M. E. O'Neill, "A 'New' Method of Identification," Journal of Criminal Law and Criminology, vol. 26, no. 4, pp. 608–610, 1935.

[4]. R. B. Hill, "Apparatus and Method for Identifying Individuals Through Their Retinal Vasculature Patterns," U.S. Patent 4109237, 1978.

[5]. R. B. Hill, "Rotating Beam Ocular Identification Apparatus and Method," U.S. Patent 4393366, 1983.

[6]. R. B. Hill, "Fovea-Centered Eye Fundus Scanner," U.S. Patent 4620318, 1986.

[7]. J. C. Johnson and R. B. Hill, "Eye Fundus Optical Scanner System and Method," U.S. Patent 5532771, 1990.

[8]. R. B. Hill, "Retina Identification", Springer US, 1996, pp. 123–141.

[9]. Z.-W. Xu, X.-X. Guo, X.-Y. Hu, and X. Cheng, "The Blood Vessel Recognition of Ocular Fundus," in International Conference on Machine Learning and Cybernetics, 2005, pp. 4493–4498.

[10]. C. Mariño, M. G. Penedo, M. Penas, M. J. Carreira, and F. Gonzalez, "Personal authentication using digital retinal images," Springer Pattern Analysis and Applications, vol. 9, no. 1, pp. 21–33, 2006.

[11]. A. Arakala, J. S. Culpepper, J. Jeffers, A. Turpin, S. Bozta ̧s, K. J. Horadam,and A. M. McKendrick, "Entropy of the Retina Template," in Advances in Biometrics, M. Tistarelli and M. S. Nixon, Eds. Springer Berlin Heidelberg, 2009, pp. 1250–1259.

[12]. M. Ortega, M. G. Penedo, J. Rouco, N. Barreira, and M. J. Carreira,"Personal verification based on extraction and characterisation of retinal feature points," Journal of Visual Languages & Computing, vol. 20, no. 2,pp. 80–90, 2009.

[13]. H. Farzin, H. Abrishami-Moghaddam, and M.-S. Moin, "A Novel Retinal Identification System," EURASIP Journal on Advances in Signal Processing, vol. 2008, p. 280635, 2008.

[14]. M. Agopov, "Retinal identification," in IntechOpen Biometrics, J. Yang,Ed., 2011, ch. 5.

[15]. W. Barkhoda, F. Akhlaqian, M. D. Amiri, and M. S. Nouroozzadeh, "Retina identification based on the pattern of blood vessels using fuzzy logic," EURASIP Journal on Advances in Signal Processing, p. 113(2011), 2011.

[16]. J. Widjaja and U. Suripon, "Retina recognition using compression-based joint transform correlator," Optical Engineering, vol. 50, no. 9, p. 098201, 2011.

[17]. M. Sabaghi, S. R. Hadianamrei, M. Fattahi, M. R. Kouchaki, and A. Zahedi, "Retinal Identification System Based on the Combination of Fourier and Wavelet Transform," Journal of Signal and Information Processing, vol. 3, pp. 35–38, 2012.

[18]. S. M. Lajevardi, A. Arakala, S. A. Davis, and K. J. Horadam, "Retina Verification System Based on Biometric Graph Matching," IEEE Transactions on Image Processing, vol. 22, no. 9, pp. 3625–3635, 2013.
[19]. M. Frucci, D. Riccio, G. S. di Baja, and L. Serino, "Using direction and score information for retina based person verification," Elsevier Expert Systems with Applications, vol. 94, pp. 1–10, 2018.
[20]. Fishman RS. Optic disc asymmetry. Arch Ophthalmol 1970;84:590-594.
[21]. I. P. Conner, J. S. Schuman, and D. L. Epstein, Examination of the Optic Nerve, chapter 8, pp. 81–94, Slack Incorporated, Thorofare, NJ, USA, 5 edition, 2013.
[22]. Quigley HA, Enger C, Katz J, Sommer R, Gilbert D. Risk factors for the development of glaucomatous visual field loss in ocular hypertension. Arch Ophthalmol 1994;112:644-649.
[23]. H. Leung, J. J. Wang, E. Rochtchina, A. G. Tan, T. Y. Wong, L. D.Hubbard, R. Klein, and P. Mitchell, "Computer-assisted retinal vessel measurement in an older population: correlation between right and left eyes," Clinical and Experimental Ophthalmology, vol. 31, pp. 326–330, 2003.
[24]. D. L. Budnez, "Symmetry Between the Right and Left Eyes of the NormalRetinal Nerve Fiber Layer Measured with Optical Coherence Tomography(An Aos Thesis)," Transactions of the American Ophthalmological Society, vol. 106, p. 252–275, 2008.
[25]. H. Li, P. R. Healey, Y. M. Tariq, E. Teber, and P. Mitchell, "Symmetry of Optic Nerve Head Parameters Measured by the Heidelberg Retina Tomograph 3 in Healthy Eyes: The Blue Mountains Eye Study," Elsevier American Journal of Ophthalmology, vol. 155, no. 3, pp. 518–523, 2013.
[26]. M. Yang, W. Wang, Q. Xu, S. Tan, and S. Wei, "Interocular symmetry of the peripapillary choroidal thickness and retinal nerve fibre layer thickness in healthy adults with isometropia," BMC Opthalmology, vol. 16, p. 182, 2016.
[27]. M. Zhou, B. Lu, J. Zhao, Q. Wang, P. Zhang, and X. Sun, "Interocular Symmetry of Macular Ganglion Cell Complex Thickness in Young Chinese Subjects," PLoS ONE, vol. 11, no. 7, 2016.
[28]. R. Mastey, M. Gaffney, K. Litts, C. Langlo, E. Patterson, M. Strampe,A. Kalitzeos, M. Michaelides, and J. Carroll, "Assessing the Interocular Symmetry of Foveal Outer Nuclear Layer Thickness in Achromatopsia," ARVO Translational Vision Science & Technology, vol. 8, no. 5, p. 21, 2019.
[29]. S. Biswas, J. Rohdin, T. Mnuk, and M. Drahansky, "Is there any similarity between a person's left and right retina?" in International Conference of the Biometrics Special Interest Group (BIOSIG), Lecture Notes in Informatics. GI -Group for computer science, 2019, pp. 71–82.
[30]. S. Biswas, J. Rohdin, M. Drahanský, "Interretinal Symmetry in Color Fundus Photographs," EMBC, 2020, pp. 1980-1983.
[31]. S. Biswas, J. Rohdin, M. Drahanský, "Bilateral Symmetry in Central Retinal Blood Vessels" IWBF, 2020, pp. 1-6.
[32]. S. Biswas, J. Rohdin, A. Kavetskyi, G. Saraiva, A. Biswas, M. Drahanský, "Investigation of Bilateral Similarity in Central Retinal Blood Vessels," IEEE Access 9, 2021 63012-63028.
[33]. S. Biswas, J. Rohdin, A. Biswas, M. Drahanský, "A Study of Bilateral Symmetry in Color Fundus Photographs," IEEE Access 9, 2021, pp. 109624-109651.
[34]. S. Biswas, J. Rohdin, and M. Drahansky, "Suitable Embedding to Find Similarity Between Left and Right Retinas of a Person," in CISP-BMEI, 2019, pp. 1–6.
[35]. H. Zhang, H. Shu, G.-N. Han, G. Coatrieux, L. Luo, J.-L. Coatrieux, "Blurred Image Recognition by Legendre Moment Invariants," IEEE Trans. Image Process. 19(3): 596-611 (2010)
[36]. Teague, M.R. (1980) Image Analysis via the General Theory of Moments. Journal of the Optical Society of America, 70, 920-930.
[37]. K.M. Hosny. Exact Legendre moment computation for gray level images. Pattern Recognition, 40(12):3597-3605, 2007.
[38]. C. G. Owen, A. R. Rudnicka, C. M. Nightingale, R. Mullen, S. A. Barman, N. Sattar, D. G. Cook, and P. H. Whincup, "Retinal arteriolar tortuosity and cardiovascular risk factors in a multi-ethnic population study of 10-year-old children; The child heart and health study in England (CHASE)," Arterioscler Thromb Vasc Biol, vol. 31, no. 8, pp. 1933–1938, 2011. Available at https://staffnet.kingston.ac.uk/~ku15565/CHASE_DB1/assets/CHASEDB1.zip
[39]. M. M. Fraz, P. Remagnino, A Hoppe, B Uyyanonvara, C. G. Owen, A. R. Rudnicka, and S. Barman, "Retinal Vessel Extraction Using First-Order Derivative of Gaussian and Morphological Processing" in Advances in Visual Computing - 7th International Symposium (ISVC), Lecture Notes in Computer Science,2011, pp. 410-420
[40]. E. Decencière, X. Zhang, G. Cazuguel, B. Lay, B. Cochener, C. Trone, P. Gain, R. Ordonez, P. Massin, A. Erginay, B. Charton, J.-C. Klein, "Feedback on a publicly distributed database: the Messidor database." Image Analysis & Stereology, v. 33, n. 3, p. 231-234, 2014. Available at: http://www.ias-iss.org/ojs/IAS/article/view/1155 or http://dx.doi.org/10.5566/ias.1155.

Md. Iqbal Aziz Khan, et. al. "Finding Similarity between the Left and Right Retinal Images of an Individual Using Legendre Moments." *IOSR Journal of Computer Engineering (IOSR-JCE)*, 23(6), 2021, pp. 29-34.